Please cite this article in press as: Chinnadurai et al., Actin Cytoskeletal Disruption following Cryopreservation Alters the Biodistribution of Human Mesenchymal Stromal Cells In Vivo, Stem Cell Reports (2014), http://dx.doi.org/10.1016/j.stemcr.2014.05.003

Stem Cell Reports
Article

ISSCR

OPEN ACCESS

Actin Cytoskeletal Disruption following Cryopreservation Alters the Biodistribution of Human Mesenchymal Stromal Cells In Vivo

Raghavan Chinnadurai,[1,2] Marco A. Garcia,[3] Yumiko Sakurai,[4,6] Wilbur A. Lam,[4,6] Allan D. Kirk,[7,8] Jacques Galipeau,[1,2,4,5] and Ian B. Copland[1,2,*]

[1]Department of Hematology and Oncology, Emory University School of Medicine, Atlanta, GA 30322, USA
[2]Winship Cancer Institute, Emory University, Atlanta, GA 30322, USA
[3]Emory Healthcare, Atlanta, GA 30322, USA
[4]Department of Pediatrics, Emory University, Atlanta, GA 30322, USA
[5]Aflac Cancer and Blood Disorders Center, Children's Healthcare of Atlanta, Atlanta, GA 30322, USA
[6]Wallace H. Coulter Department of Biomedical Engineering, Georgia Tech and Emory University, Atlanta, GA 30322, USA
[7]Department of Surgery, Division of Transplantation, Emory University School of Medicine, Atlanta, GA 30322, USA
[8]Emory Transplant Center, Emory University, Atlanta, GA 30322, USA
*Correspondence: ian.copland@emory.edu
http://dx.doi.org/10.1016/j.stemcr.2014.05.003

SUMMARY

Mesenchymal stromal cells have shown clinical promise; however, variations in treatment responses are an ongoing concern. We previously demonstrated that MSCs are functionally stunned after thawing. Here, we investigated whether this cryopreservation/thawing defect also impacts the postinfusion biodistribution properties of MSCs. Under both static and physiologic flow, compared with live MSCs in active culture, MSCs thawed from cryopreservation bound poorly to fibronectin (40% reduction) and human endothelial cells (80% reduction), respectively. This reduction correlated with a reduced cytoskeletal F-actin content in post-thaw MSCs (60% reduction). In vivo, live human MSCs could be detected in murine lung tissues for up to 24 hr, whereas thawed MSCs were undetectable. Similarly, live MSCs whose actin cytoskeleton was chemically disrupted were undetectable at 24 hr postinfusion. Our data suggest that post-thaw cryopreserved MSCs are distinct from live MSCs. This distinction could significantly affect the utility of MSCs as a cellular therapeutic.

INTRODUCTION

Mesenchymal stromal cells (MSCs) are a promising cellular therapeutic for numerous disorders because of their anti-inflammatory/regenerative properties and the fact that they are readily expandable ex vivo (Copland and Galipeau, 2011). However, discrepancies in the therapeutic effectiveness of these cells as determined in phase II/III trials have called into question their therapeutic utility (Galipeau, 2013). A common practice in many MSC immunotherapy trials is to expand MSCs ex vivo and then cryogenically bank them until needed. The MSCs are then thawed and administered within a couple of hours to the patient. Until recently, the assumption was that viable post-thaw MSCs have physiological features comparable to those of their noncryopreserved counterparts. We have found that this premise may be flawed. Previously, we demonstrated that cryopreserved MSCs (cryo MSCs) have a blunted indoleamine 2,3-dioxygenase (IDO) response immediately post-thaw, which significantly reduced their immunomodulatory activity (François et al., 2012). In support of this idea are experimental data showing that when renal allograft recipients are treated with the IDO inhibitor 1-methyl-tryptophan or with IDO-deficient MSCs, tolerance is not established (Ge et al., 2010). Thus, MSCs must retain their capacity to make IDO to evoke an immunosuppressive effect.

For MSCs to have an immunosuppressive effect, they must not only actively respond to inflammatory cues but also persist/engraft within the body (Huang et al., 2010; Richardson et al., 2013; Sarkar et al., 2011). Systemic infusion of MSCs in nonhuman primates demonstrated that MSCs can take up residence in many tissues (Devine et al., 2003), but upon sensing an injury signal, MSCs will home to areas of inflammation (Li et al., 2002). Whether the means by which MSCs are prepared for administration impacts their homing/engraftment potential has not been rigorously evaluated. However, Castelo-Branco et al. (2012) demonstrated that transfused cryo MSCs could not migrate to an inflamed colon and had no beneficial effect in a 2,4,6-trinitrobenzenesulfonic acid (TNBS)-induced colitis model. This suggests that cryo MSCs may have an engraftment defect. In our efforts to optimize the therapeutic utility of MSCs, we compared the in vitro and in vivo binding/engraftment potential of human MSCs (hMSCs) thawed from cryopreservation with that of MSCs in active culture.

RESULTS

Cryo hMSCs Show Attenuated Binding in Static and Flow Conditions In Vitro

Previously, we demonstrated that cryo MSCs are functionally stunned immediately after thawing (François et al.,

Please cite this article in press as: Chinnadurai et al., Actin Cytoskeletal Disruption following Cryopreservation Alters the Biodistribution of Human Mesenchymal Stromal Cells In Vivo, Stem Cell Reports (2014), http://dx.doi.org/10.1016/j.stemcr.2014.05.003

2012). Here, to further elucidate the extent to which cryopreservation impacts the functional properties of MSCs, we compared the binding potential of cells thawed from cryopreservation (cryo MSCs) with that of cells harvested from active culture (live MSCs) in vitro. Based on trypan blue exclusion of early passage (p3–5) MSCs from five different donors, viability was 92% ± 2.51% when they were in active culture; however, immediately post-thaw, there was a small but significant reduction in viability to 87% ± 2.76% (Figure 1A). This reduction in viability post-thaw was even more apparent when we utilized Annexin V/propidium iodide (PI) staining (Figure 1B), which can better discriminate between cells that are live (Annexin V−/PI−) or in early apoptosis (Annexin V+/PI−), mid–late apoptosis (Annexin V+/PI+), or necrosis (Annexin V−/PI+). In a paired comparison of five unique MSC donors, we noted that the percentage of MSCs in apoptosis was always higher in the cryo MSCs compared with their paired live MSC counterparts (Figure 1C). Thus, MSC viability was reduced immediately after thawing; however, the degree of reduction varied substantially depending on the assay employed. Because of the discrepancy between our trypan blue and Annexin V/PI staining results, we chose to rely on trypan blue exclusion in the remaining experiments to normalize the total number of viable cells for comparison of cryo and live MSCs. The rationale for this was based on two lines of thought: first, Annexin V/PI staining can produce false-positive signals (Rieger et al., 2010), and second, trypan blue is the most commonly used method to evaluate MSC viability clinically (see Discussion for more detailed comments). Next, we investigated whether MSC-integrin-based binding to extracellular matrix was altered post-thaw. Under static conditions, viable PHK26-labeled cryo or live MSCs were seeded onto fibronectin-coated plates at 5,000 cells/cm^2 and allowed to attach for 2 hr at 37°C in a 5% CO_2 incubator. Qualitatively, there was a clear reduction in the number of bound cryo MSCs compared with live MSCs (Figure 1D). Quantitatively, using both standard hemocytometer cell counting (data not shown) and the flow-cytometric method described in Experimental Procedures, we found that cryo MSCs had a significant reduction in binding capacity to fibronectin relative to live MSCs (live 100.00% ± 5.61% versus cryo 60.06% ± 5.64; Figure 1E). This binding defect was even more pronounced when cryo MSCs were exposed to vascular flow conditions. Specifically, by utilizing a three-dimensional endothelialized fluidic system (Tsai et al., 2013; Figure 1F), we infused cryo and live MSCs at a rate equivalent to 2 dynes/cm^2 into the microfluidic device for 1 hr and observed a profound difference in the ability of Cyro MSCs to bind to endothelial cells compared with live MSCs (live MSCs 6.3 ± 0.9/channel versus cryo MSCs 1.3 ± 0.3/channel; Figure 1G).

Cryo hMSCs Show Attenuated Engraftment in the Lungs In Vivo

Because no in vitro system can fully recapitulate the complexities of in vivo cell adhesion, migration, and homing, we next evaluated the engraftment potential of hMSCs in C57BL/B6 mice. In order to track hMSCs in vivo, we infused hMSCs from a male donor into female mice and measured the relative engraftment of MSCs by measuring the male Y-chromosome SRY gene by real-time PCR (Figure S1A available online). By performing in vitro mixing experiments using combinations of male hMSCs with female mouse splenocytes, we established a highly sensitive human SRY detection limit of one male hMSC in 200 mouse cells (0.5% frequency; Figure S1B). Feasibility experiments demonstrated that intravenous infusion of male hMSCs into female mice resulted in SRY gene detection exclusively within the lungs as early as 5 min postinfusion (Figure S1C). Biodistribution and kinetics experiments using multiple unique hMSC populations infused into mice demonstrated that at 24 hr, hMSCs could be readily detected within the lungs, but by 3 days the hMSCs could no longer be identified in the lungs (Figure 2A) or in any other organs tested (Figure S2). Based on these data, we selected MSC engraftment in the lung at 24 hr postinfusion as a surrogate to compare and contrast the in vivo binding potential of cryo MSCs immediately post-thaw with that of live MSCs. Consistent with our in vitro data, we found that cryo MSCs, from two separate donors, had significantly reduced lung engraftment as compared with their live MSC counterparts (cycle of threshold $[CT]^{-1}_{cryo} = 0.030 \pm 0.0020$;$CT^{-1}_{live} = 0.034 \pm 0.0032$;$CT^{-1}_{NoMSC} = 0.029 \pm 0.0021$; Figure 2B). To validate our SRY gene readout, we reproduced these findings using a human-specific genomic DNA (gDNA) primer set and showed that there was again a significant difference in hMSC engraftment between live and cryo MSCs ($CT^{-1}_{cryo} = 0.029 \pm 0.0022$;$CT^{-1}_{live} = 0.033 \pm 0.0020$;$CT^{-1}_{NoMSC} = 0.028 \pm 0.0016$), whereas there was no difference in signal when mouse lung gDNA was tested using a mouse-specific gDNA primer set (Figures 2C and 2D).

Dead Cells in the Infusion Mixture Neither Bind Nor Influence Lung Homing of Live MSCs In Vivo

Both our trypan blue and Annexin V/PI viability data suggested that an increase in the number of dead and/or dying cells might explain some of our data; however, it is unknown whether dead cells can modulate the engraftment of live cells. To resolve this issue, we infused a mixture of live and dead hMSCs into the animals. hMSCs from a male individual were heat killed and mixed with live MSCs from a female MSC donor at a ratio of 1:1 (Figure 3A). The infusion mixture was then subjected to SRY and total human gDNA real-time PCR to ensure that SRY

Please cite this article in press as: Chinnadurai et al., Actin Cytoskeletal Disruption following Cryopreservation Alters the Biodistribution of Human Mesenchymal Stromal Cells In Vivo, Stem Cell Reports (2014), http://dx.doi.org/10.1016/j.stemcr.2014.05.003

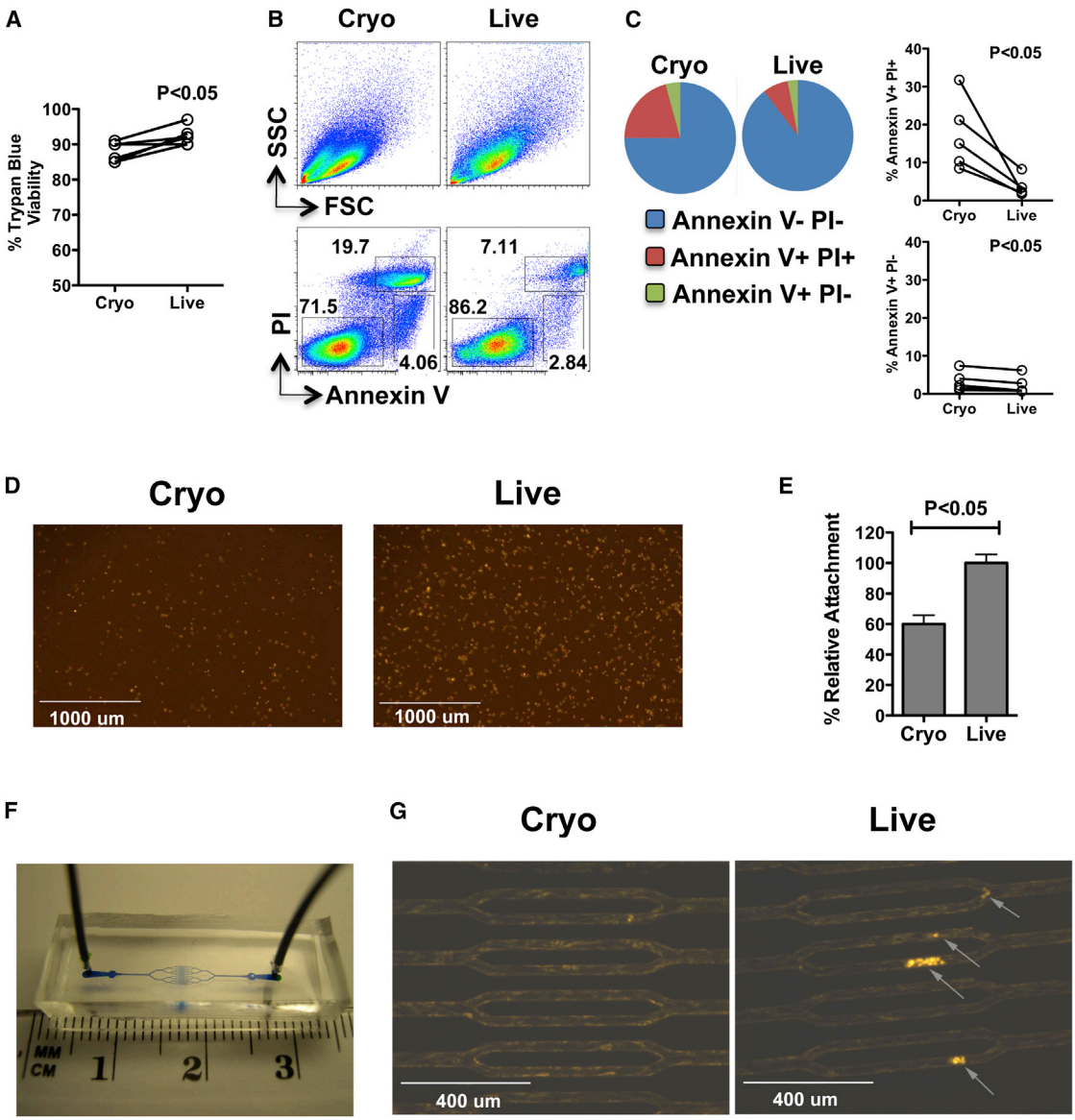

Figure 1. Cryo hMSCs Show Attenuated Binding In Vitro under Both Static and Flow Conditions

(A) Cumulative trypan blue cell viability counts of cryo versus live MSCs from five independent experiments using five unique MSC donors.

(B) MSCs thawed from cryopreservation (cryo MSCs) or in active culture (live MSCs) were subjected to Annexin V/PI staining and acquired by flow cytometry. The top panel shows the forward scatter/side scatter profile and the bottom panel shows Annexin V/PI staining representations of cryo and live MSC populations.

(C) Pie diagram showing the relative frequencies of Annexin V−/PI−, Annexin V+/PI+, and Annexin V+/PI− populations, as well as cumulative Annexin V−/PI−, Annexin V+/PI+, and Annexin V+/PI− frequencies from five independent experiments using five unique donors.

(D and E) Cryo and live MSCs were labeled with the fluorescent dye PKH26 and seeded onto plates coated with fibronectin. Two hours later, unbound cells were washed off the plates and cell adherence was measured (D) qualitatively by microscopy and (E) quantitatively by flow cytometry.

(F) Macroscopic view of the microfluidic flow chamber.

(G) Endothelial cell-coated microchannels were infused (2 dynes/cm^2) with fluorescently labeled cryo and live MSCs. One hour after infusion, the bound MSCs were measured by fluorescence microscopy. For trypan blue and Annexin V/PI, individual viability numbers are shown; relative cell attachment is shown as cumulative mean ± SD based on three independent experiments using three unique MSC donors. A p value < 0.05 was considered statistically significant based on two-tailed t tests.

Please cite this article in press as: Chinnadurai et al., Actin Cytoskeletal Disruption following Cryopreservation Alters the Biodistribution of Human Mesenchymal Stromal Cells In Vivo, Stem Cell Reports (2014), http://dx.doi.org/10.1016/j.stemcr.2014.05.003

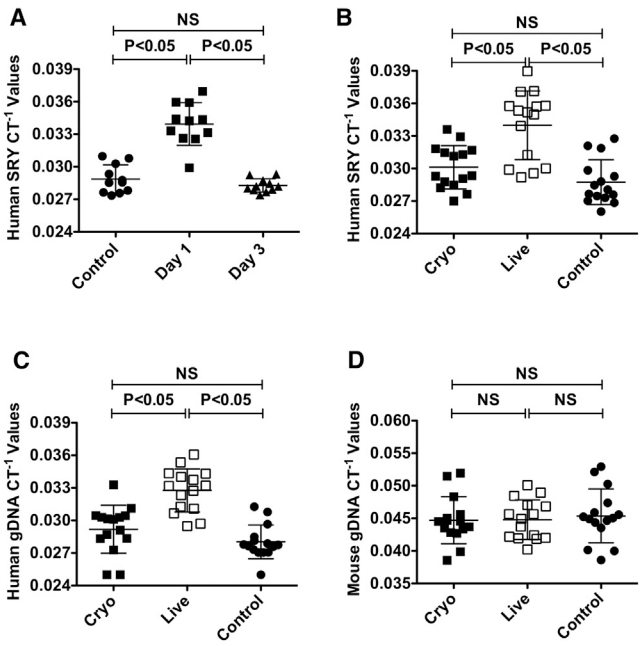

Figure 2. Cryo hMSCs Show Attenuated Engraftment In Vivo

(A) Human male MSCs (1×10^6) were injected intravenously into female C57BL/B6 mice through the tail vein. The animals were sacrificed at the indicated time points and the lungs were collected for gDNA extraction and SRY real-time PCR.

(B–D) Viable cryo or live hMSCs (1×10^6) were injected into the tail vein of C57BL/B6 mice. At 24 hr postinfusion, the animals were sacrificed and the lungs were excised to extract total gDNA for real-time PCR amplification of (B) human SRY, (C) human gDNA, and (D) mouse gDNA. CT^{-1} values are shown on the y axis. Individual CT^{-1} values and the cumulative mean ± SD from two to three independent experiments (n = 5 or 6 animals per group) performed with two unique MSC donors are shown. A p value < 0.05 was considered statistically significant based on one-way ANOVA and Tukey's multiple comparison test.

See also Figures S1 and S2.

could be detected in the dead cells (Figure S3). Mice infused with both live (female) and dead (male) or live (female) and live (male) MSC mixtures were sacrificed 24 hr postinjection. Our results clearly demonstrate that dead cells do not engraft in the lungs (Figures 3B and 3C; $SRYCT^{-1}_{\text{female-live male-live}} = 0.031 \pm 0.0021$; $SRYCT^{-1}_{\text{female-live male-dead}} = 0.028 \pm 0.00054$) and do not alter the engraftment of live cells when they are part of the infusion mixture ($SRYCT^{-1}_{\text{male-live\_female-live}} = 0.031 \pm 0.0021$; $SRYCT^{-1}_{\text{male-live\_female-dead}} = 0.031 \pm 0.0011$; Figures 3D and 3E).

Cryopreservation Does Not Alter Adhesion Molecule Expression on MSCs

It was previously demonstrated that hematopoietic stem cells (HSCs) shed L-selectin (CD62L) upon thawing after cryopreservation (De Boer et al., 1998; Koenigsmann et al., 1998). Consequently, we investigated whether the attenuated binding potential of MSCs could be explained by changes in the surface expression of adhesion molecules on MSCs after cryopreservation. Using flow cytometry, we evaluated the expression level of various cell-surface molecules, including tetraspanin (CD63), Integrin alpha V (CD51), MHC class I (HLA-ABC), Integrin beta 1(CD29), Integrin alpha 4 (CD49d), Integrin alpha IIb (CD41), ICAM 1 (CD54), Integrin beta 3 (CD61), and Integrin alpha 5 (CD49e). Compared with their isotype controls (Figure 4A, gray histograms), MSCs showed surface expression (Figure 4A, open histograms) of CD63, CD51, HLA-ABC, CD29, CD49d, CD61, and CD49e, but did not show strong expression of CD41 or CD54 (Figure 1A). For the markers evaluated, there were no obvious differences in the cell-surface expression patterns of paired live and cryo MSC donors (n = 2), suggesting that cryo MSCs do not shed their adhesion molecules during the cryopreservation and thawing process (Figures 4A and 4B). Consistent with these data, there was no difference in the surface expression of the SDF-1 chemokine receptor CXCR4 between live and cryo MSCs (data not shown).

Cryo MSCs Exhibit Metabolic Activities Similar to Those of Live MSCs

An alternative explanation for the reduced binding of cryo MSCs could relate to their metabolic fitness. Previously, the ability of a cell to evoke a calcium influx was shown to mediate monocyte adhesion to endothelial cells (Himi et al., 2012); therefore, we measured the ability of cryo and live MSCs to take up extracellular calcium. Incubating cryo and live MSCs with a fluorescent Ca^{+2} indicator demonstrated no difference between cryo and live MSCs with regard to their kinetic uptake of the fluorescent Ca^{+2} indicator (Figures 5A and 5B). Similarly, when we measured the metabolic activity of live and cryo MSCs based on their ability to reduce the viability dye PrestoBlue, we found no difference between the two groups regardless of seeding density (% PrestoBlue reduction: live MSCs 73% ± 5% and cryo MSCs 78% ± 7% at the highest seeding density; Figure 5C).

Cryopreservation Disrupts Actin Polymerization and Limits the Engraftment of MSCs in Vivo

Because there were no obvious cell-surface or metabolic defects that could explain the reduced binding of cryo MSCs, we evaluated the ability of MSCs to form F-actin, as cryopreservation was previously shown to alter the actin cytoskeleton in both fibroblasts and MSCs (Ragoonanan et al., 2010; Xu et al., 2012). Both cryo and live MSCs were seeded onto fibronectin-coated plates for 2 hr. Unbound cells were then washed off and attached cells were

Please cite this article in press as: Chinnadurai et al., Actin Cytoskeletal Disruption following Cryopreservation Alters the Biodistribution of Human Mesenchymal Stromal Cells In Vivo, Stem Cell Reports (2014), http://dx.doi.org/10.1016/j.stemcr.2014.05.003

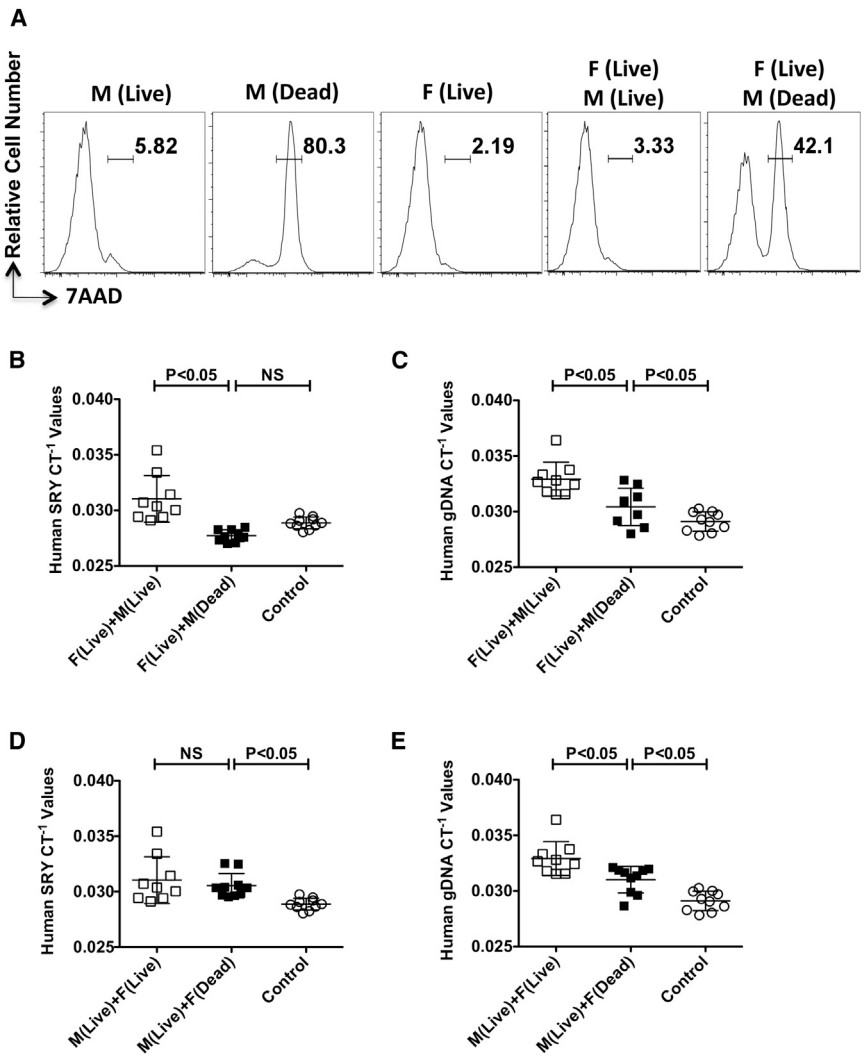

Figure 3. Dead MSCs in the Infusion Mixture Do Not Engraft In Vivo and Do Not Influence Engraftment of Live MSCs In Vivo

(A) 7AAD viability staining of MSCs that were live, heat killed, or a combination of the two.

(B and C) Male MSCs (1×10^6) live or heat killed (dead), were mixed with live MSCs derived from a female donor at a ratio of 1:1 (0.5×10^6 each) and then injected intravenously into C57BL/B6 mice via the tail vein. At 24 hr postinfusion, the animals were sacrificed and the lungs were excised to extract total gDNA for real-time PCR amplification of (B) SRY and (C) human gDNA.

(D and E) Female MSCs (1×10^6) live or heat killed (dead), were mixed with live MSCs derived from a male donor at a ratio of 1:1 (0.5×10^6 each) and then injected intravenously into C57BL/B6 mice via the tail vein. At 24 hr postinfusion, the animals were sacrificed and the lungs were excised to extract total gDNA for real-time PCR amplification of (D) SRY and (E) human gDNA. Individual CT^{-1} values and the cumulative mean ± SD from two independent experiments (n = 4–5 animals per group) performed with male and female MSC donors are shown. A p value < 0.05 was considered statistically significant based on two-tailed t tests.

See also Figure S3.

stained with fluorescein isothiocyanate (FITC)-conjugated phalloidin to visualize F-actin microscopically. Compared with live MSCs, the abundance and organization of F-actin in cryo MSCs was qualitatively different (Figure 6A). On a per cell basis, quantitatively, F-actin content was significantly lower in Cyro MSCs than in their live MSC counterparts (Figure 6B). These data suggested that defective F-actin polymerization may explain the reduced binding capacity of cryo MSCs. Therefore, we tested whether disruption of F-actin could influence the engraftment potential of MSCs in vivo. We chemically disrupted F-actin of live MSCs with 2 μM of Cytochalasin D for 2 hr prior to infusion. Consistent with prior reports (Yourek et al., 2007), a 2 hr incubation with 2 μM of Cytochalasin D effectively disrupted F-actin (Figure 6C), but did not cause significant cell death (Figures 6D and S4). Intravenous infusion of 1×10^6 control (DMSO-treated) or Cytochalasin D-treated MSCs into C57BL/B6 animals demonstrated that at 24 hr postinfusion, animals that were infused with Cytochalasin D-treated MSCs had significantly fewer MSCs in the lung than the control live MSCs ($CT^{-1}{}_{live}$ = 0.033 ± 0.0022; $CT^{-1}{}_{CytochalasinD}$ = 0.031 ± 0.0025; Figure 6E), whereas the loading control mouse gDNA CT^{-1} values were similar (Figure 6F).

Culture Rescue of MSCs Post-Thaw Restores Their In Vivo Biodistribution Potential

Previously, we demonstrated that the immunosuppressive functionality of MSCs could be restored post-thaw by a short culture recovery period (François et al., 2012). Here, in a final investigation, we determined whether a similar culture recovery could restore MSCs' engraftment potential post-thaw. Using two separated hMSC donors, we injected C57BL/B6 mice via the tail vein with 1×10^6 MSCs that were live (cultured for >7 days), cryo (thawed the day of infusion), or Recovered (48 hr culture post-thaw). At

Please cite this article in press as: Chinnadurai et al., Actin Cytoskeletal Disruption following Cryopreservation Alters the Biodistribution of Human Mesenchymal Stromal Cells In Vivo, Stem Cell Reports (2014), http://dx.doi.org/10.1016/j.stemcr.2014.05.003

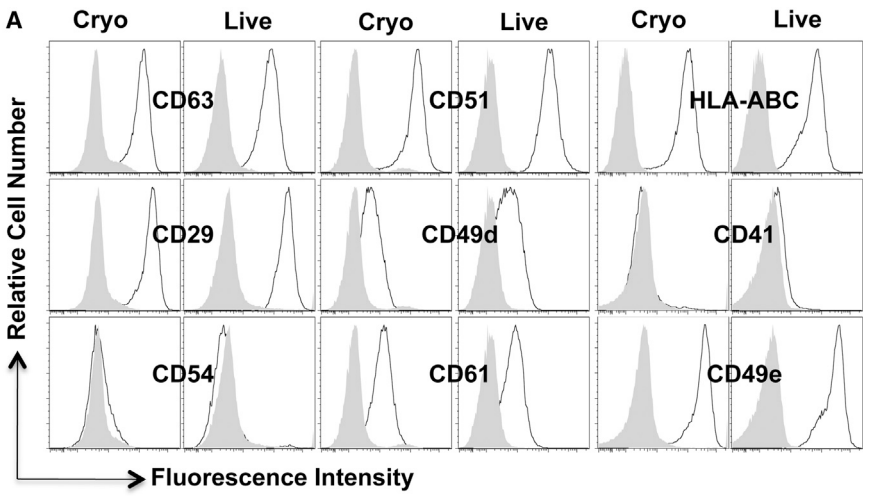

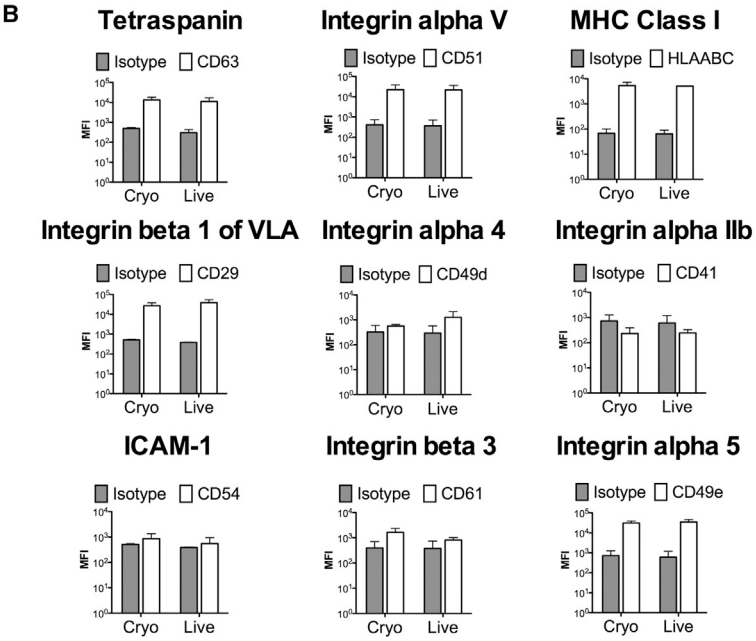

Figure 4. Cryopreservation Does Not Alter the Expression of Adhesion Molecules on MSCs

(A) Flow-cytometric analysis of the adhesion molecules tetraspanin (CD63), Integrin alpha V (CD51), MHC class I (HLA-ABC), Integrin beta 1 (CD29), Integrin alpha 4 (CD49d), Integrin alpha IIb (CD41), ICAM1 (CD54), Integrin beta 3 (CD61), and Integrin alpha 5 (CD49e) on live or cryo MSCs. Open histograms represent the adhesion molecule expression and gray histograms represent the appropriate isotype control.

(B) Cumulative mean fluorescent intensity (MFI) of adhesion marker expression as the average mean ± SD from two independent experiments using two unique MSC donors.

24 hr postinfusion, the lungs were excised and human gDNA real-time PCR was performed to quantify the engraftment of MSCs. Our results clearly demonstrate that a 48 hr culture recovery corrects the immediate post-thaw in vivo binding defect we observe in hMSCs (CT^{-1}_{cryo} = 0.028 ± 0.00066; CT^{-1}_{48hr} = 0.030 ± 0.0012; CT^{-1}_{live} = 0.030 ± 0.00083; $CT\text{-}1_{control}$ = 0.027+0.00082; Figures 7A and 7B).

DISCUSSION

Large-scale expansion and cryopreservation of MSCs is an attractive option from a clinical delivery perspective. Manufacturing large lots of a therapeutic provides a degree of consistency, economy of scale, and reduced regulatory burden with regard to lot testing and release criteria. Furthermore, the ability to thaw a product and infuse it within a short time frame provides an approach that is convenient and requires neither specialized equipment nor extensive personnel training to perform. However, unless the prefreeze functionality of the product is preserved post-thaw, the cost savings and convenience benefits will be outweighed by the prospect of reduced therapeutic potency. In the present study, we expand on our previous observations that cryopreservation attenuates the immunosuppressive capacity of MSCs by demonstrating that

Please cite this article in press as: Chinnadurai et al., Actin Cytoskeletal Disruption following Cryopreservation Alters the Biodistribution of Human Mesenchymal Stromal Cells In Vivo, Stem Cell Reports (2014), http://dx.doi.org/10.1016/j.stemcr.2014.05.003

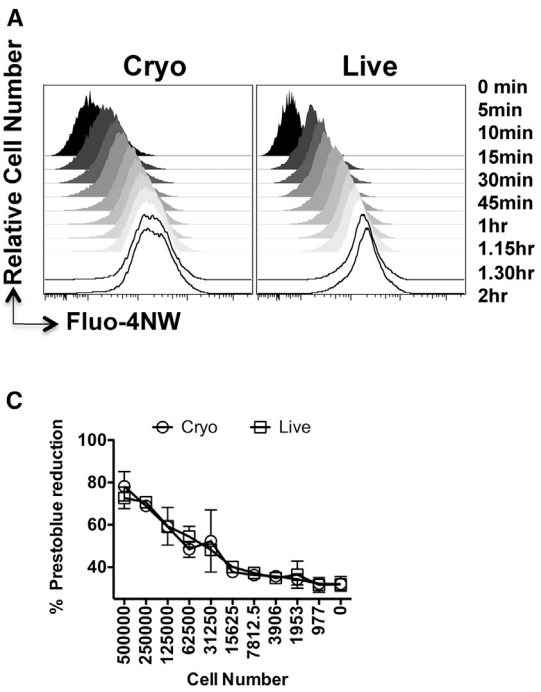

Figure 5. Cryo MSCs Exhibit Metabolic Activities Similar to Those of Live MSCs

(A) Relative fluorescence of MSCs incubated with the calcium influx indicator Fluo-NW at the indicated time points as measured by flow cytometry.

(B) Fluo-NW MFI between cryo and live MSCs at the indicated time points.

(C) Comparison of PrestoBlue dye (Invitrogen) reduction of cryo and live MSCs at varying seeding densities. Representative results from two independent experiments performed on two unique MSC donors are shown.

cryo MSCs have attenuated binding and engraftment potential immediately post-thaw.

The homing/engraftment of MSCs is the process by which cells migrate, engraft, and exert local functional effects. Homing involves a cascade of events initiated by shear-resistant adhesive interactions between flowing cells and the target endothelium or extracellular matrix. This process is mediated by adhesion receptors expressed on circulating cells that engage relevant coreceptors, resulting in cell tethering, rolling, and firm adherence (Sackstein, 2005). Similarly to induction of IDO in MSCs, we demonstrate that homing/engraftment of MSCs is an "active" process that requires cells that are metabolically (i.e., viable) and functionally fit, as dead MSCs or those with a disrupted actin cytoskeleton do not engraft. We demonstrate that immediately after thawing, cryo MSCs have a reduced capacity to bind to both extracellular matrix molecules (i.e., fibronectin) and endothelial cells, and these binding defects can be reproduced in vivo. Consistent with our data, Castelo-Branco et al. (2012) showed that cryo MSCs are incapable of homing to the inflamed colon in a murine model of colitis, and Hattori et al. (2001) showed that HSCs also have a migratory defect post-thaw. Thus, we propose that the process of cryopreservation and thawing exerts a generic negative effect on cells with regard to their migratory/homing properties.

Cryoinjury is a significant problem in many primary cell types (Durkut et al., 2013; Fortunato et al., 2013) and is likely associated with both generic and cell-specific effects. Within the mesenchymal lineage, both hMSCs (François et al., 2012) and human primary fibroblasts (Liu et al., 2000) undergo a biochemical "heat-shock stress response" when thawed from cryopreservation, which not only serves to protect the cells from death (Beere, 2005; Yenari et al., 2005) but can also result in protein synthesis inhibition (Cuesta et al., 2000; Doerwald et al., 2003). Conversely, although both HSCs and MSCs have a reduced binding potential post-thaw, mechanistically the defect appears to be cell-type dependent. For HSCs, the primary defect appears to be due to shedding of L-selectin from the membrane (De Boer et al., 1998; Koenigsmann et al., 1998) and is due primarily to DMSO exposure rather than the freezing process. Selectins comprise a family of three members (E-, P-, and L-selectin), are differentially expressed by leukocytes and endothelial cells, and are involved in the early steps of leukocyte extravasation. There is no evidence from the literature that MSCs possess selectins (Rüster et al., 2006); thus, shedding of selectin is unlikely to explain our result. On the other hand, MSCs do express numerous cell adhesion molecules, including VLA4 (CD49d and CD29 integrins) (De Ugarte et al., 2003), that can interact with VCAM-1 on endothelial cells. As such, we investigated whether receptor shedding of nonselectin adhesion receptors might explain the defect we observed. Our data suggested that receptor shedding is unlikely to be the putative cause for reduced MSC binding immediately post-thaw. Furthermore, we ruled out viability, calcium influx, and metabolism as possible explanations. Thus, the homing defect in MSCs that occurs immediately after thawing is not only different from

Please cite this article in press as: Chinnadurai et al., Actin Cytoskeletal Disruption following Cryopreservation Alters the Biodistribution of Human Mesenchymal Stromal Cells In Vivo, Stem Cell Reports (2014), http://dx.doi.org/10.1016/j.stemcr.2014.05.003

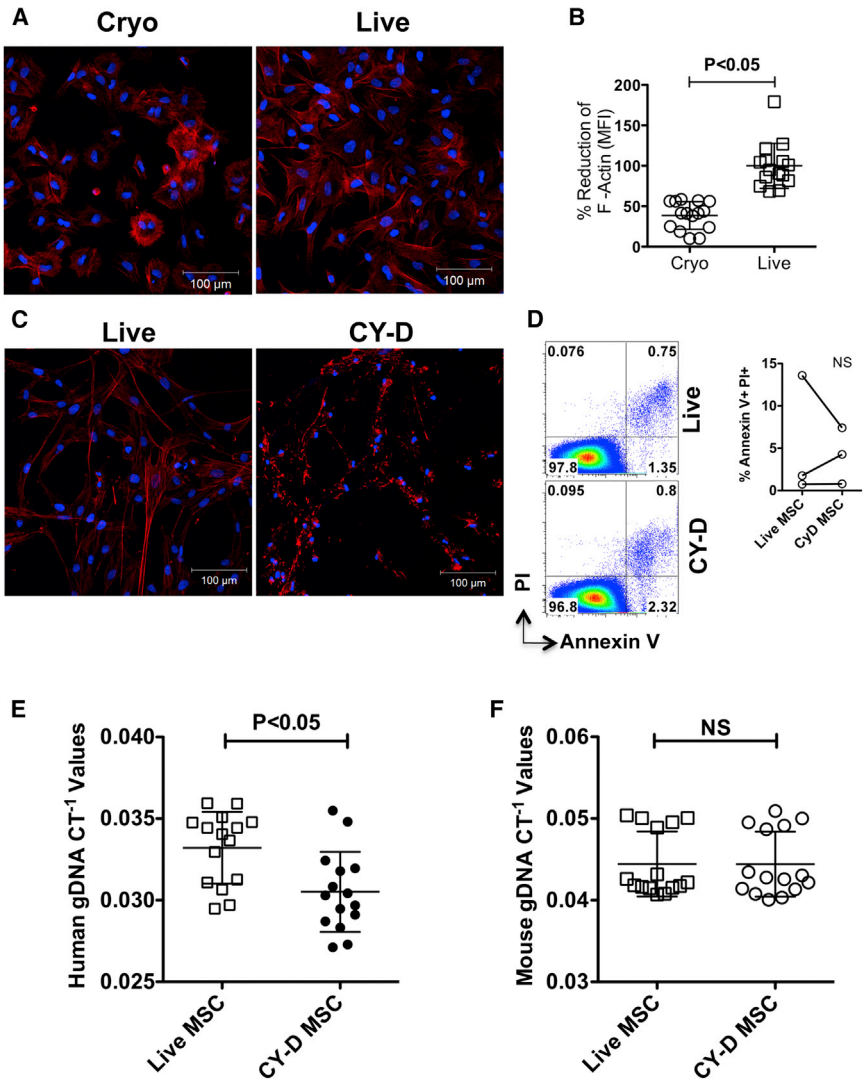

Figure 6. Cryo MSCs Show Defective F-Actin Polymerization Compared with Live MSCs

(A) MSCs thawed from cryopreservation (cryo MSCs) or MSCs trypsinized out of the flasks from the incubator (live MSCs) were seeded onto fibronectin-coated glass coverslips. Two hours after attachment, cells were fixed with formalin and stained for F-actin (red, phalloidin conjugated with Alexa 555) and nuclei (blue, DAPI). Images were taken using a Zeiss microscope at 20× magnification.

(B) Percentage reduction of F-actin MFI in cryo MSCs compared with live MSCs.

(C) Nontreated MSCs and MSCs treated with Cytochalasin D (2 μM) for 2 hr were seeded onto fibronectin-coated glass coverslips and then stained for F-actin (red) and DAPI (blue).

(D) Cytochalasin D-treated MSCs and non-treated MSCs were trypsinized, subjected to Annexin V/PI staining, and analyzed by flow cytometry.

(E and F) MSCs (1×10^6) with or without Cytochalasin D treatment were injected intravenously into C57BL/B6 mice via the tail vein. At 24 hr postinfusion, the animals were sacrificed and the lungs were excised to extract total gDNA for real-time PCR amplification of (E) human gDNA and (F) mouse gDNA. In vitro F-actin quantification is shown as the cumulative mean ± SD based on the averaged signal of at least five unique fields from two independent experiments with two separate MSCs donors. In vivo individual CT^{-1} values and the cumulative mean ± SD from three independent experiments (n = 4–5 animals per group) performed with two unique MSC donors are shown. A p value < 0.05 was considered statistically significant based on two-tailed t tests.

See also Figure S4.

that seen in HSCs but is also independent of basal metabolism.

Although the mechanical properties of adhesive attachments are usually attributed to the ligand-receptor interaction, the strength and survival of cell attachment depend heavily on molecular connections below the plasma membrane surface (Evans and Calderwood, 2007). In particular, the interactions of the cytoplasmic integrin b tails with intracellular cytoskeletal and signaling proteins figure prominently in the regulation of integrin activation (Evans and Calderwood, 2007). Furthermore, efficient actin polymerization organization and remodeling are critically important for stabilizing integrin ligand interactions, which allows cells to resist detachment under conditions of flow (Rullo et al., 2012). Recently, Xu et al. (2012) evaluated the effect of cooling rates on the recovery of MSCs from cryopreservation and demonstrated that immediately after thawing, the F-actin component of the cytoskeletons was disrupted. They further demonstrated that the critical process that led to the changes in F-actin morphology and distribution was not the addition/removal of the cryopreservative (i.e., DMSO), but rather the freezing process itself, and that slower cooling rates of 5°C/min and 10°C/min resulted in greater disruption (Xu et al., 2012). In another study, Ragoonanan et al. (2010) demonstrated that post-thaw cryo MSCs show abnormal actin morphology as well as changes in intracellular pH and mitochondrial aggregation. This prompted us to

Please cite this article in press as: Chinnadurai et al., Actin Cytoskeletal Disruption following Cryopreservation Alters the Biodistribution of Human Mesenchymal Stromal Cells In Vivo, Stem Cell Reports (2014), http://dx.doi.org/10.1016/j.stemcr.2014.05.003

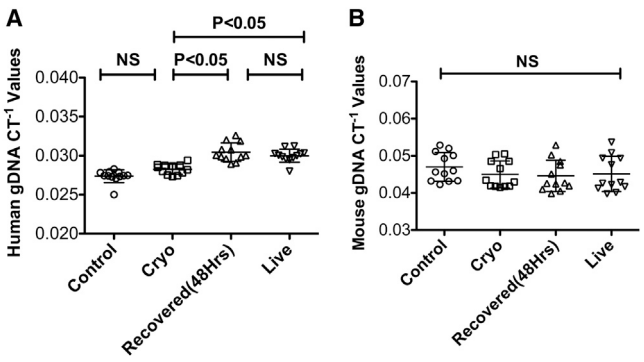

Figure 7. Culture Rescue of MSCs after Thawing Restores Their In Vivo Biodistribution Potential

(A and B) Thawed (cryo), 48 hr culture-rescued (Recovered 48 hr), or 7 day cultured (live) MSCs (1×10^6) were injected intravenously into C57BL/B6 mice via the tail vein. At 24 hr postinfusion, the animals were sacrificed and the lungs were excised to extract total gDNA for real-time PCR amplification of (A) human gDNA and (B) mouse gDNA. Individual CT^{-1} values and the cumulative mean ± SD from two independent experiments (n = 5 and 7 animals per group, respectively) performed with two unique MSC donors are shown. A p value < 0.05 was considered statistically significant based on one-way ANOVA and Tukey's multiple comparison tests.

investigate the F-actin polymerization capabilities of MSCs in our system. In agreement with the above reports, we found that (1) immediately after thawing, cryo MSCs had a significantly reduced capacity to polymerize F-actin in vitro, and (2) when the F-actin cytoskeleton of cultured live MSCs was chemically disrupted, they lost their capacity to engraft in vivo. Thus, the ability of MSCs to rapidly remodel their cytoskeleton is a significant contributor to the homing/engraftment defect we observed. Other possible contributors to the MSC binding defect we observed include alterations in integrin confirmation or clustering that could impact binding affinity or avidity, respectively, as well as alterations in the formation of macromolecular adhesion complexes that could impact signal transduction. However, these were not evaluated in this study. In future studies, understanding how cryopreservation and thawing affects the intra- and extracellular binding machinery of MSCs, and developing strategies to mitigate these binding defects may help to improve the therapeutic utility of MSCs and minimize potential safety issues.

In addition to demonstrating how the cryopreservation and thawing process impacts the binding characteristics of MSCs, we observed that viability can vary substantially depending on the assay employed. In this work, we utilized several methods to determine cell viability, which yielded different results. As shown in Figure 1, we compared the results from trypan blue exclusion and Annexin V/PI staining, and in both assays we noted that post-thaw MSCs had reduced viability compared with their live counterparts; however, the values obtained with trypan blue and Annexin V/PI were substantially different. We attribute these differences to the different sensitivities and specificities of the respective assays. Trypan blue exclusion is by far the most commonly used method to assess viability because it is easily performed, generally has a low false-positive rate, and requires only a hemocytometer and microscope. Unfortunately, trypan blue is not particularly sensitive and can be subject to interoperator variability and yield ambiguous or conflicting results. Conversely, Annexin V/PI staining is very sensitive and can discriminate between cells at various stages of the cell-death spectrum. However, the Annexin V/PI assay can also produce significant false-positive signals. Specifically, PI has the potential to bind to RNA in the cytosol (Rieger et al., 2010), and there are multiple examples of cells that are Annexin V positive do not actually undergo apoptosis because the translocation of phosphatidylserine to the cell surface is a reversible process (Kenis et al., 2010; van den Eijnde et al., 2001). Furthermore, because DMSO is known to induce transient pores (Gurtovenko and Anwar, 2007; He et al., 2012; Notman et al., 2006) it is possible that a significant, nonspecific influx of both Annexin V and PI occurred in our MSCs post-thaw. Given the false-positive potential of Annexin V/PI, we chose to normalize our seeding and infusion experiments based on trypan blue viability. Because we used trypan blue versus Annexin V/PI to normalize for live cells, we feel confident that viability differences between the two methods did not unduly influence the data or our interpretation. This assertion is based on the data generated for Figure 3, which show that even when 50% dead cells were infused, we could still reliably detect live cells at 24 hr postinfusion.

To date, the prevailing concept has been that viability and functionality are directly linked; however, our findings argue that viability does not equate to functionality. To help mitigate the impact of cryopreservation on MSCs, several studies have aimed to enhance the quality of the infused product by improving viability post-thaw using various cryopreservation/thawing techniques (Haack-Sørensen and Kastrup, 2011; Lee et al., 2012; Li et al., 2013; Pravdyuk et al., 2013). Although they achieved some improvements in viability, none of these studies evaluated the functional capacity of their MSCs post-thaw, and it is unclear whether a small change in viability would equate to meaningful differences in functionality. These data are particularly relevant to trials that employ allogeneic MSCs. von Bahr et al. (2012) recently analyzed autopsy tissues from 18 patients who had received allogeneic MSC therapy, and demonstrated that infusion did not result in ectopic tissue formation. In addition, PCR analysis

Please cite this article in press as: Chinnadurai et al., Actin Cytoskeletal Disruption following Cryopreservation Alters the Biodistribution of Human Mesenchymal Stromal Cells In Vivo, Stem Cell Reports (2014), http://dx.doi.org/10.1016/j.stemcr.2014.05.003

of MSC donor DNA showed that MSC engraftment could be detected in patients early on, but with time, engraftment became scarce. These data suggest that there is limited long-term engraftment of allogeneic MSCs. It is now well established that allogeneic MSCs do evoke an immune response in vivo (Eliopoulos et al., 2005), and this response can be classified as acute/innate (Crop et al., 2011) or acquired (Eliopoulos et al., 2005; Poncelet et al., 2007). In the case of an acute/innate effect, Moll et al. (2012) demonstrated that allogeneic MSCs can evoke an instant blood-mediated inflammatory reaction (IBMIR), which can result in a rapid loss of up to 80% of the infused cells, similar to what has been observed after allogeneic hepatocyte transplantation (Gustafson et al., 2011). Furthermore, Moll et al. (2014) recently demonstrated that the IBMIR response to MSCs is intensified when cryo MSCs are tested in vitro shortly after thawing. Whether this IBMIR response occurs in both the allogeneic and autologous MSC settings remains to be established; however, one would predict that regardless of the source of the cells, the IBMIR response would likely be accentuated immediately after thawing from cryopreservation. Thus, to really optimize the cryopreservation and thawing process of MSCs for therapeutic purposes, one must independently evaluate the viability, functionality, and potential immunogenicity (IBMIR) of these cells. Until such time as a cryopreservation and thawing procedure can yield a viable and fully functional MSC product immediately after thawing, our data support the idea of using live MSCs rather than post-thaw cryo MSCs for clinical evaluation of MSCs as an immunosuppressive agent.

EXPERIMENTAL PROCEDURES

MSC Isolation and Culture

hMSCs were isolated from bone marrow aspirates collected from the iliac crest of consenting subjects (Emory University IRB00046063) as previously described (Copland et al., 2013). After the third passage, the MSC cultures were assayed by flow-cytometric analysis for the absence of CD45+ and CD34+ contaminating cells and expression of CD44, CD73, CD90, and CD105 (BD Bioscience).

Cell Viability

Cell viability was evaluated using trypan blue exclusion and Annexin V/PI or 7-AAD staining, and quantified by either standard hemocytometry (trypan blue) or fluorescence-activated cell sorting (FACS) analysis (Annexin V/PI or 7-AAD).

Cryopreservation and Thawing of MSCs

Subconfluent MSCs were trypsinized, washed, resuspended in freezing media at a concentration of 5×10^6 cells/ml, and then placed in a freezing container (Nalgene Mr. Frosty; Sigma). When they reached −80°C, the MSCs were transferred to liquid nitrogen for cryostorage. For thawing, the MSCs were removed from the liquid nitrogen, quickly thawed (1–2 min), and then immediately transferred into MSC complete medium for centrifugation at 1,600 rpm for 5 min. The pelleted MSCs were resuspended in MSC complete medium and recentrifuged prior to viability assessment and enumeration.

Flow Cytometry

Annexin V/PI staining (Invitrogen) and calcium influx assay (Fluo-4 NW calcium assay kit; Molecular Probes) were performed and acquired via flow cytometry according to the manufacturers' instructions. Cell-surface adhesion molecule profiling of MSCs was performed with antibodies to CD63, CD51, HLA-ABC, CD29, CD49d, CD41, CD54, CD61, and CD49e (Biolegend). All data were collected on a BD FACSCanto II system (Becton Dickinson).

Cell-Binding Assay in the Static Condition

Live or cryo MSCs were labeled with the fluorescent dye PKH26 (Sigma) and seeded onto fibronectin-coated plates at 5,000 cells/cm^2. Two hours after seeding, the unbound cells were removed from the plates and attached cells were imaged by epifluorescence microscopy using an EVOS FL Cell Imaging System. For quantitative measurements, the attached cells were trypsinized and enumerated using either a hemocytometer or flow cytometry. For flow-cytometry enumeration, pelleted cells from each condition were resuspended in equivalent volumes and a BD FACSCanto II (Becton Dickinson) was programmed to collect events for 60 s. Based on the fluorescently gated cell population, the number of events recorded correlated with the relative cell number. Relative cell adherence was then expressed as a percentage, with live MSCs counts normalized to 100%.

Microfluidics Flow System

The design and fabrication of three-dimensional in vitro "endothelialized" microvasculature models were described previously (Tsai et al., 2012). The microchannels were coated with 50 μg/ml fibronectin from human plasma (Sigma) and then incubated at 37°C, 5% CO_2, for 1 hr. Endothelial cells were prepared at a concentration of 500,000 cells/ml in Endothelial Growth Medium-2 (EGM-2; Lonza) with 8% mass/vol of dextran 500 (Sigma). Endothelial cells were manually preloaded into the inlet tubing and infused into the channels with a syringe pump at 1.25 ml/min for 2 hr, and then perfused with EGM-2 at the same rate for 2–3 days. Live or cryo MSCs were labeled with carboxyfluorescein succinimidyl ester to render them fluorescent and then suspended at 1×10^6 cells/ml in EGM-2. Following syringe loading, the MSCs were pumped through the microchannels for 1 hr at 1.25 ml/min. Epifluorescence and bright-field microscopy were acquired following the experiment using an EVOS FL Cell Imaging System.

PrestoBlue Dye Reduction

Live or cryo MSCs were seeded onto a 96-well plate at the appropriate density. PrestoBlue cell viability reagent (Life Technologies) was added, and at 3 hr postincubation the plates were read at 570 nm and 600 nm wavelengths to determine absorbance. The percent reduction of PrestoBlue reagent was calculated according to the manufacturer's instructions.

Please cite this article in press as: Chinnadurai et al., Actin Cytoskeletal Disruption following Cryopreservation Alters the Biodistribution of Human Mesenchymal Stromal Cells In Vivo, Stem Cell Reports (2014), http://dx.doi.org/10.1016/j.stemcr.2014.05.003

Infusion into Animals and gDNA Preparation

Animal experiments were carried out in accordance with the guidelines an Institutional Animal Care and Use Committee. The protocol was approved by the Committee on the Ethics of Animal Experiments of Emory University. MSCs were prepared at a concentration of 1×10^6 total viable cells based on trypan blue exclusion in infusion media (0.5% human albumin in PBS) and then loaded into a syringe. C57BL/B6 mice (8–10 weeks old; The Jackson Laboratories) were injected intravenously with MSCs via a tail vein. The mice were euthanized in a CO_2 chamber at the indicated time points postinfusion to collect the specified organs. The QIAamp DNA Mini Kit (QIAGEN) was used to extract DNA from the tissues. Briefly, 25 mg of the organs was weighed and lysed using a Proteinase K solution and then placed on QIAamp Mini spin columns to extract gDNA according to the manufacturer's instruction. The extracted DNA was quantified using the Epoch Micro-Volume Spectrophotometer System (Biotek) according to the manufacturer's protocol.

Quantitative Real-Time PCR

For gDNA PCR, 100 ng of total DNA was used as a template for 25 ml of reaction mix containing RT^2 SYBR Green ROX qPCR master mix (QIAGEN) and either the mouse RT^2 qPCR primer gDNA control primer set (QIAGEN), human SRY RT^2 qPCR primer set (QIAGEN), or the RT^2 qPCR primer assay for human gDNA contamination (Cat. No. PA-031; SA Biosciences). An Applied Biosystem 7500 fast real-time PCR system was used to perform the standard PCR cycle procedure to identify the CT values. The CT values are expressed as an inverse (CT^{-1}) to better graphically represent increases or decreases in expression.

Heat Killing and Cytochalasin D Treatment of MSCs

hMSCs (10×10^6) were resuspended in 0.5% human albumin (CSL Behring LLC) in PBS at a concentration of 5×10^6 cells/ml. The resuspended cells were placed on a 56°C heating block for 30 min and then placed on ice before they were mixed with live cells at a 1:1 ratio. Adherent MSCs were treated with Cytochalasin D (Sigma) at a concentration of 2 μM for 2 hr at 37°C in a 5% CO_2 incubator. After incubation, the cells were washed in complete medium and trypsinized. The cells were washed, counted, and adjusted to a final concentration of 5×10^6 viable cells/ml in 0.5% human albumin in PBS.

F-Actin Staining

Fibronectin-coated coverslips were seeded with cryo, live, or Cytochalasin D-treated MSCs at similar concentrations. At 2 hr postincubation, unbound cells were washed away. The cells were fixed with 10% formalin (Fisher Scientific) for 10 min. The fixed cells were washed three times with PBS. F-actin and nuclei were stained with phalloidin conjugated with Alexa 555 (Molecular Probes, Invitrogen) and DAPI (Molecular Probes, Invitrogen). The stained cells were imaged with a Zeiss LSM 510 microscope. Images were analyzed with the use of Zeiss ZEN 2009 software.

Statistical Analysis

Data were analyzed with GraphPad Prism 5.0 software. An unpaired two-sided t test was used to determine significance between the means of two groups, and a one-way ANOVA with Tukey's multiple comparison test was used to compare multiple groups simultaneously. A p value < 0.05 was considered statistically significant.

SUPPLEMENTAL INFORMATION

Supplemental Information includes four figures and can be found with this article online at http://dx.doi.org/10.1016/j.stemcr.2014.05.003.

ACKNOWLEDGMENTS

We thank Shala Yuan, Jordan Murphy, and Deborah Martinson for technical assistance and the Emory Personalized Immunotherapy Center (EPIC) for providing hMSCs and platelet lysate reagents. This study was supported by a Georgia Cancer Coalition Award to J.G. and a Robbins Scholar Award to I.B.C. Part of this research was performed as a project for the Immune Tolerance Network (NIH contract N01 AI15416), supported by the National Institute of Allergy and Infectious Diseases. This research project was also supported in part by the Emory University Integrated Cellular Imaging Microscopy Core of the Winship Cancer Institute comprehensive cancer center grant P30CA138292.

Received: November 28, 2013
Revised: May 5, 2014
Accepted: May 6, 2014
Published: June 5, 2014

REFERENCES

Beere, H.M. (2005). Death versus survival: functional interaction between the apoptotic and stress-inducible heat shock protein pathways. J. Clin. Invest. *115*, 2633–2639.

Castelo-Branco, M.T., Soares, I.D., Lopes, D.V., Buongusto, F., Martinusso, C.A., do Rosario, A., Jr., Souza, S.A., Gutfilen, B., Fonseca, L.M., Elia, C., et al. (2012). Intraperitoneal but not intravenous cryopreserved mesenchymal stromal cells home to the inflamed colon and ameliorate experimental colitis. PLoS ONE *7*, e33360.

Copland, I.B., and Galipeau, J. (2011). Death and inflammation following somatic cell transplantation. Semin. Immunopathol. *33*, 535–550.

Copland, I.B., Garcia, M.A., Waller, E.K., Roback, J.D., and Galipeau, J. (2013). The effect of platelet lysate fibrinogen on the functionality of MSCs in immunotherapy. Biomaterials *34*, 7840–7850.

Crop, M.J., Korevaar, S.S., de Kuiper, R., IJzermans, J.N., van Besouw, N.M., Baan, C.C., Weimar, W., and Hoogduijn, M.J. (2011). Human mesenchymal stem cells are susceptible to lysis by CD8(+) T cells and NK cells. Cell Transplant. *20*, 1547–1559.

Cuesta, R., Laroia, G., and Schneider, R.J. (2000). Chaperone hsp27 inhibits translation during heat shock by binding eIF4G and facilitating dissociation of cap-initiation complexes. Genes Dev. *14*, 1460–1470.

De Boer, F., Dräger, A.M., Van der Wall, E., Pinedo, H.M., and Schuurhuis, G.J. (1998). Changes in L-selectin expression on

CD34-positive cells upon cryopreservation of peripheral blood stem cell transplants. Bone Marrow Transplant. *22*, 1103–1110.

De Ugarte, D.A., Alfonso, Z., Zuk, P.A., Elbarbary, A., Zhu, M., Ashjian, P., Benhaim, P., Hedrick, M.H., and Fraser, J.K. (2003). Differential expression of stem cell mobilization-associated molecules on multi-lineage cells from adipose tissue and bone marrow. Immunol. Lett. *89*, 267–270.

Devine, S.M., Cobbs, C., Jennings, M., Bartholomew, A., and Hoffman, R. (2003). Mesenchymal stem cells distribute to a wide range of tissues following systemic infusion into nonhuman primates. Blood *101*, 2999–3001.

Doerwald, L., Onnekink, C., van Genesen, S.T., de Jong, W.W., and Lubsen, N.H. (2003). Translational thermotolerance provided by small heat shock proteins is limited to cap-dependent initiation and inhibited by 2-aminopurine. J. Biol. Chem. *278*, 49743–49750.

Durkut, S., Elçin, A.E., and Elçin, Y.M. (2013). In vitro evaluation of encapsulated primary rat hepatocytes pre- and post-cryopreservation at -80°C and in liquid nitrogen. Artif Cells Nanomed Biotechnol. http://dx.doi.org/10.3109/21691401.2013.837476.

Eliopoulos, N., Stagg, J., Lejeune, L., Pommey, S., and Galipeau, J. (2005). Allogeneic marrow stromal cells are immune rejected by MHC class I- and class II-mismatched recipient mice. Blood *106*, 4057–4065.

Evans, E.A., and Calderwood, D.A. (2007). Forces and bond dynamics in cell adhesion. Science *316*, 1148–1153.

Fortunato, A., Leo, R., and Liguori, F. (2013). Effects of cryostorage on human sperm chromatin integrity. Zygote *21*, 330–336.

François, M., Copland, I.B., Yuan, S., Romieu-Mourez, R., Waller, E.K., and Galipeau, J. (2012). Cryopreserved mesenchymal stromal cells display impaired immunosuppressive properties as a result of heat-shock response and impaired interferon-γ licensing. Cytotherapy *14*, 147–152.

Galipeau, J. (2013). The mesenchymal stromal cells dilemma—does a negative phase III trial of random donor mesenchymal stromal cells in steroid-resistant graft-versus-host disease represent a death knell or a bump in the road? Cytotherapy *15*, 2–8.

Ge, W., Jiang, J., Arp, J., Liu, W., Garcia, B., and Wang, H. (2010). Regulatory T-cell generation and kidney allograft tolerance induced by mesenchymal stem cells associated with indoleamine 2,3-dioxygenase expression. Transplantation *90*, 1312–1320.

Gurtovenko, A.A., and Anwar, J. (2007). Modulating the structure and properties of cell membranes: the molecular mechanism of action of dimethyl sulfoxide. J. Phys. Chem. B *111*, 10453–10460.

Gustafson, E.K., Elgue, G., Hughes, R.D., Mitry, R.R., Sanchez, J., Haglund, U., Meurling, S., Dhawan, A., Korsgren, O., and Nilsson, B. (2011). The instant blood-mediated inflammatory reaction characterized in hepatocyte transplantation. Transplantation *91*, 632–638.

Haack-Sørensen, M., and Kastrup, J. (2011). Cryopreservation and revival of mesenchymal stromal cells. Methods Mol. Biol. *698*, 161–174.

Hattori, Y., Kato, H., Nitta, M., and Takamoto, S. (2001). Decrease of L-selectin expression on human CD34+ cells on freeze-thawing and rapid recovery with short-term incubation. Exp. Hematol. *29*, 114–122.

He, F., Liu, W., Zheng, S., Zhou, L., Ye, B., and Qi, Z. (2012). Ion transport through dimethyl sulfoxide (DMSO) induced transient water pores in cell membranes. Mol. Membr. Biol. *29*, 107–113.

Himi, N., Hamaguchi, A., Hashimoto, K., Koga, T., Narita, K., and Miyamoto, O. (2012). Calcium influx through the TRPV1 channel of endothelial cells (ECs) correlates with a stronger adhesion between monocytes and ECs. Adv. Med. Sci. *57*, 224–229.

Huang, J., Zhang, Z., Guo, J., Ni, A., Deb, A., Zhang, L., Mirotsou, M., Pratt, R.E., and Dzau, V.J. (2010). Genetic modification of mesenchymal stem cells overexpressing CCR1 increases cell viability, migration, engraftment, and capillary density in the injured myocardium. Circ. Res. *106*, 1753–1762.

Kenis, H., Zandbergen, H.R., Hofstra, L., Petrov, A.D., Dumont, E.A., Blankenberg, F.D., Haider, N., Bitsch, N., Gijbels, M., Verjans, J.W., et al. (2010). Annexin A5 uptake in ischemic myocardium: demonstration of reversible phosphatidylserine externalization and feasibility of radionuclide imaging. J. Nucl. Med. *51*, 259–267.

Koenigsmann, M.P., Koenigsmann, M., Notter, M., Neuloh, M., Mücke, C., Thiel, E., and Berdel, W.E. (1998). Adhesion molecules on peripheral blood-derived CD34+ cells: effects of cryopreservation and short-term ex vivo incubation with serum and cytokines. Bone Marrow Transplant. *22*, 1077–1085.

Lee, S.Y., Huang, G.W., Shiung, J.N., Huang, Y.H., Jeng, J.H., Kuo, T.F., Yang, J.C., and Yang, W.C. (2012). Magnetic cryopreservation for dental pulp stem cells. Cells Tissues Organs (Print) *196*, 23–33.

Li, Y., Chen, J., Chen, X.G., Wang, L., Gautam, S.C., Xu, Y.X., Katakowski, M., Zhang, L.J., Lu, M., Janakiraman, N., and Chopp, M. (2002). Human marrow stromal cell therapy for stroke in rat: neurotrophins and functional recovery. Neurology *59*, 514–523.

Li, Q., Wang, Y., and Deng, Z. (2013). Pre-conditioned mesenchymal stem cells: a better way for cell-based therapy. Stem Cell Res Ther *4*, 63.

Liu, K., Yang, Y., and Mansbridge, J. (2000). Comparison of the stress response to cryopreservation in monolayer and three-dimensional human fibroblast cultures: stress proteins, MAP kinases, and growth factor gene expression. Tissue Eng. *6*, 539–554.

Moll, G., Rasmusson-Duprez, I., von Bahr, L., Connolly-Andersen, A.M., Elgue, G., Funke, L., Hamad, O.A., Lönnies, H., Magnusson, P.U., Sanchez, J., et al. (2012). Are therapeutic human mesenchymal stromal cells compatible with human blood? Stem Cells *30*, 1565–1574.

Moll, G., Hult, A., von Bahr, L., Alm, J.J., Heldring, N., Hamad, O.A., Stenbeck-Funke, L., Larsson, S., Teramura, Y., Roelofs, H., et al. (2014). Do ABO blood group antigens hamper the therapeutic efficacy of mesenchymal stromal cells? PLoS ONE *9*, e85040.

Notman, R., Noro, M., O'Malley, B., and Anwar, J. (2006). Molecular basis for dimethylsulfoxide (DMSO) action on lipid membranes. J. Am. Chem. Soc. *128*, 13982–13983.

Poncelet, A.J., Vercruysse, J., Saliez, A., and Gianello, P. (2007). Although pig allogeneic mesenchymal stem cells are not immunogenic in vitro, intracardiac injection elicits an immune response in vivo. Transplantation *83*, 783–790.

Pravdyuk, A.I., Petrenko, Y.A., Fuller, B.J., and Petrenko, A.Y. (2013). Cryopreservation of alginate encapsulated mesenchymal stromal cells. Cryobiology *66*, 215–222.

Ragoonanan, V., Hubel, A., and Aksan, A. (2010). Response of the cell membrane-cytoskeleton complex to osmotic and freeze/thaw stresses. Cryobiology *61*, 335–344.

Richardson, J.D., Nelson, A.J., Zannettino, A.C., Gronthos, S., Worthley, S.G., and Psaltis, P.J. (2013). Optimization of the cardiovascular therapeutic properties of mesenchymal stromal/stem cells-taking the next step. Stem Cell Rev. *9*, 281–302.

Rieger, A.M., Hall, B.E., Luong, T., Schang, L.M., and Barreda, D.R. (2010). Conventional apoptosis assays using propidium iodide generate a significant number of false positives that prevent accurate assessment of cell death. J. Immunol. Methods *358*, 81–92.

Rullo, J., Becker, H., Hyduk, S.J., Wong, J.C., Digby, G., Arora, P.D., Cano, A.P., Hartwig, J., McCulloch, C.A., and Cybulsky, M.I. (2012). Actin polymerization stabilizes α4β1 integrin anchors that mediate monocyte adhesion. J. Cell Biol. *197*, 115–129.

Rüster, B., Göttig, S., Ludwig, R.J., Bistrian, R., Müller, S., Seifried, E., Gille, J., and Henschler, R. (2006). Mesenchymal stem cells display coordinated rolling and adhesion behavior on endothelial cells. Blood *108*, 3938–3944.

Sackstein, R. (2005). The lymphocyte homing receptors: gatekeepers of the multistep paradigm. Curr. Opin. Hematol. *12*, 444–450.

Sarkar, D., Spencer, J.A., Phillips, J.A., Zhao, W., Schafer, S., Spelke, D.P., Mortensen, L.J., Ruiz, J.P., Vemula, P.K., Sridharan, R., et al. (2011). Engineered cell homing. Blood *118*, e184–e191.

Tsai, M., Kita, A., Leach, J., Rounsevell, R., Huang, J.N., Moake, J., Ware, R.E., Fletcher, D.A., and Lam, W.A. (2012). In vitro modeling of the microvascular occlusion and thrombosis that occur in hematologic diseases using microfluidic technology. J. Clin. Invest. *122*, 408–418.

Tsai, H.E., Liu, G.S., Kung, M.L., Liu, L.F., Wu, J.C., Tang, C.H., Huang, C.H., Chen, S.C., Lam, H.C., Wu, C.S., and Tai, M.H. (2013). Downregulation of hepatoma-derived growth factor contributes to retarded lung metastasis via inhibition of epithelial-mesenchymal transition by systemic POMC gene delivery in melanoma. Mol. Cancer Ther. *12*, 1016–1025.

van den Eijnde, S.M., van den Hoff, M.J., Reutelingsperger, C.P., van Heerde, W.L., Henfling, M.E., Vermeij-Keers, C., Schutte, B., Borgers, M., and Ramaekers, F.C. (2001). Transient expression of phosphatidylserine at cell-cell contact areas is required for myotube formation. J. Cell Sci. *114*, 3631–3642.

von Bahr, L., Batsis, I., Moll, G., Hägg, M., Szakos, A., Sundberg, B., Uzunel, M., Ringden, O., and Le Blanc, K. (2012). Analysis of tissues following mesenchymal stromal cell therapy in humans indicates limited long-term engraftment and no ectopic tissue formation. Stem Cells *30*, 1575–1578.

Xu, X., Liu, Y., Cui, Z., Wei, Y., and Zhang, L. (2012). Effects of osmotic and cold shock on adherent human mesenchymal stem cells during cryopreservation. J. Biotechnol. *162*, 224–231.

Yenari, M.A., Liu, J., Zheng, Z., Vexler, Z.S., Lee, J.E., and Giffard, R.G. (2005). Antiapoptotic and anti-inflammatory mechanisms of heat-shock protein protection. Ann. N Y Acad. Sci. *1053*, 74–83.

Yourek, G., Hussain, M.A., and Mao, J.J. (2007). Cytoskeletal changes of mesenchymal stem cells during differentiation. ASAIO J. *53*, 219–228.